

Raman study of phonons in Chevrel-phase crystals

D. J. Holmgren, R. T. Demers, M. V. Klein, and D. M. Ginsberg

*Department of Physics and Materials Research Laboratory, University of Illinois at Urbana-Champaign,
1110 West Green Street, Urbana, Illinois 61801*

(Received 16 March 1987)

We have grown single crystals of the Chevrel-phase compounds $\text{Cu}_{1.8}\text{Mo}_6\text{S}_8$, $\text{Cu}_{3.2}\text{Mo}_6\text{S}_8$, PbMo_6S_8 , BaMo_6S_8 , and SnMo_6S_8 . Vibrational Raman spectra of these crystals were obtained to determine energies and symmetries of zone-center phonons. Where they overlap, these measured energies are in agreement with tunnel-junction-measured phonon energies. Covering a higher and wider range of frequencies, the Raman data are complementary to the tunneling data. The energies of the Raman-active phonons are roughly independent of the particular metal atom in the compound.

I. INTRODUCTION

The Chevrel-phase compounds are ternary molybdenum chalcogenides, with compositions $A_x\text{Mo}_6\text{C}_8$, where A is a metal or rare-earth ion and C is a chalcogen (S, Se, or Te).^{1,2} These materials have received considerable attention in the last 15 years because of the high values displayed by some of the compounds for the superconducting transition temperature T_c and the upper critical field H_{c2} . The superconducting behavior varies considerably for different atoms A . The electronic and the phonon structure of the compounds determine the superconducting properties.

Much progress has been made towards understanding the electronic band structure of the Chevrel phases.³⁻⁵ The band structure is dominated by effects of the cluster structure of the compounds. The Mo_6C_8 clusters are also thought to play a very important role in determining the lattice dynamics of the Chevrel-phase compounds. A molecular-crystal model has been proposed.⁶ It states that the normal modes of the unit cell fall into two categories: the "internal" modes, involving only relative motions of the atoms within the cluster, and "external" modes, involving motions of the quasirigid cluster and the metal atoms. Heat-capacity,^{7,8} neutron scattering,^{6,9,10} and Mössbauer^{11,12} measurements are consistent with this model. Arguments by Bader and Sinha¹³ indicate that although the molecular-crystal model is not correct in a rigorous sense, it is useful for gaining insight into the lattice dynamics.

With the exception of $\text{Cu}_2\text{Mo}_6\text{S}_8$ and Mo_6Se_8 acoustic phonon dispersion data,¹⁰ the available neutron scattering data describe only the phonon density of states. Superconducting tunneling measurements have been published,^{14,15} which include phonon structure information. These data indicate the positions of the lower energy peaks weighted by the electron-phonon interaction in the phonon density of states and are in good agreement with the neutron data. No results have been reported on the characteristics of individual optical phonons.

In this paper we report the growth of single crystals of the superconducting Chevrel-phase compounds PbMo_6S_8 ,

SnMo_6S_8 , $\text{Cu}_{1.8}\text{Mo}_6\text{S}_8$, and $\text{Cu}_{3.2}\text{Mo}_6\text{S}_8$, and the nonsuperconducting BaMo_6S_8 . We have obtained the vibrational Raman spectra of these crystals to determine the energies and symmetries of zone-center phonons.

II. STRUCTURE AND SYMMETRY

The sulfur Chevrel-phase structure is best described as being built by the stacking of Mo_6S_8 blocks. These clusters consist of sulfur structures which are nearly cubic, surrounding Mo octahedra. The clusters are arranged on a rhombohedral lattice and are twisted by about 27° around the ternary axis. The metal atoms A_x of $A_x\text{Mo}_6\text{S}_8$ go into the roughly cubic cavities formed between the clusters.

At room temperature, the standard "large atom"² Chevrel-phase structure, $A\text{Mo}_6\text{S}_8$ (one metal atom per unit cell), belongs to the $R\bar{3}$ space group. A factor group analysis reveals that only half of the 42 zone-center optical modes are Raman active. The Raman active modes consists of seven doubly degenerate E_g and seven A_g modes. Table I lists the atoms of the unit cell by their site symmetry and their contributions to the Raman active optical modes.

The metal atom is not involved in any Raman active modes because of its location at a center of inversion symmetry. The sulfur atoms on the ternary axis, referred to as the axial sulfur atoms, have site symmetry C_3 . Correlation techniques reveal that the axial S atoms move only along the ternary axis in A_g modes and only in directions normal to the ternary axis in E_g modes. The remaining sulfur atoms and the molybdenum atoms contribute to both the E_g and A_g modes and it is impossible to identify the eigenvectors from a simple group theoretical analysis.

In the Chevrel-phase compounds like $\text{Cu}_{1.8}\text{Mo}_6\text{S}_8$, the metal atoms are displaced from the inversion center, so modes involving motions of these atoms may be Raman active. Moreover, the number of metal atoms per unit cell in these "small atom"² compounds varies throughout the lattice. This breaking of translational symmetry might activate phonons throughout the Brillouin zone; no such effect, however, was observed by us.

TABLE I. Atoms of the rhombohedral unit cell listed by site symmetry. Axial sulfur atoms labeled S_{11} . Nonaxial sulfur atoms labeled S_1 . Third column lists the representations of the Raman active modes.

| Atom | Raman active modes | |
|-----------|--------------------|---------------|
| | Site symmetry | Mode symmetry |
| $2S_{11}$ | C_3 | $A_g + E_g$ |
| $6S_1$ | C_1 | $3A_g + 3E_g$ |
| $6Mo$ | C_1 | $3A_g + 3E_g$ |
| M | C_{3i} | |

III. EXPERIMENT

A. Single-crystal growth

The starting materials for the single crystal growth of $PbMo_6S_8$, $BaMo_6S_8$, $SnMo_6S_8$, $Cu_{1.8}Mo_6S_8$, and $Cu_{3.2}Mo_6S_8$ were pure polycrystalline slugs of these materials with masses of about 1.6 g. These slugs were prepared with Cu, Mo, S, PbS, and SnS powders. Cu powder rather than the metal sulfide was chosen because we could not obtain water-free CuS. Details of the polycrystalline sample preparation have been reported elsewhere.^{16,17}

Each of the polycrystalline sample batches was characterized by powder x-ray diffraction. Filtered Cu $K\alpha$ radiation was used on a Philips diffractometer. No impurity phases were detected within a detection limit of about 0.1 wt. %.

Single crystals were prepared by using both vapor growth and melt techniques. For the former, a 1.55 g sintered slug was sealed in a quartz ampule (8 mm i.d., 10 cm length). The ampule was placed in a three-zone furnace. The end of the ampule containing the slug was held at 1200°C, and the other end was held at 1100°C. After approximately 100 hours, cubic crystals, about 0.5 mm on a side, were found at the cool end.

Larger crystals were grown by melting the slugs. We constructed and used a pressurized induction furnace similar to that described by Flukiger *et al.*¹⁸ This furnace has been described elsewhere.¹⁷ In a typical crystal growing experiment, between 1.5 and 5 g of sintered Chevrel-phase compound were placed in a cylindrical Al_2O_3 (Coors) or ZrO_2 (McDanel) crucible. A conical Al_2O_3 or ZrO_2 (McDanel) crucible was used as a tight-fitting cap. The crucibles were sealed with a high-temperature zirconia-based cement (Aremco). We found that this procedure was necessary when melting $SnMo_6S_8$ and $PbMo_6S_8$ to prevent the loss of Sn and Pb. Alumina crucibles were used when the temperature did not go above 1620°C. (Such crucibles react with the cement at higher temperatures.) Alumina crucibles could also be used when melting the $Cu_xMo_6S_8$ samples, as these did not need to be sealed to prevent loss of Cu. All runs above 1620°C requiring sealed crucibles were performed with zirconia crucibles.

The crucibles were heated in the furnace under 25 atm of ultrapure argon to 10 or 20°C above the melting point and then cooled at a rate of 3°C/min to 1500°C. The rf

power was then turned off, resulting in an initial cooling rate of about 150°C/min. Melting points for the $Cu_{1.8}Mo_6S_8$, $Cu_{3.2}Mo_6S_8$, $SnMo_6S_8$, $BaMo_6S_8$, and $PbMo_6S_8$ were 1735, 1735, 1625, 1665 and 1595°C, respectively (all temperatures $\pm 25^\circ C$).

Using this technique, we prepared crystals ranging in volume from 1 mm³ for the $SnMo_6S_8$, $BaMo_6S_8$, and $PbMo_6S_8$ to as much as 500 mm³ for the $Cu_xMo_6S_8$. The larger crystals always had cracks, which were probably the results of stresses during cooling. Uncracked crystals were limited in size to about 5 mm³. For the Raman measurements we required $Cu_{1.8}Mo_6S_8$ crystals that were cubic in shape and about 1 mm on a side. We found that extended annealing of our melted slugs at 1200°C produced such crystals by the separation of crystal grains at cracks and grain boundaries. This technique is much easier and less destructive than spark cutting.

B. Raman experiments

Raman spectra were excited with 514-nm or 488-nm light from an argon ion laser. The linearly polarized laser light was focused on the sample at an angle of incidence of approximately 70°, close to the pseudo-Brewster's angle, in order to maximize transmission efficiency. The laser power was typically less than 200 mW to avoid damage to the sample surface. The scattered light was collected along a direction normal to the surface and was dispersed with a 0.85-m Spex double monochromator in series with a third monochromator for additional stray light rejection. The instrumental resolution was (3.5 ± 0.5) cm⁻¹. The scattered light was analyzed by a low-loss polarizing cube and detected by a low dark count photomultiplier tube. Dwell times ran from 40 to 60 sec.

The preferred orientation for light scattering in these compounds requires the incoming radiation to be incident on the rhombohedral (111) crystal faces. Natural cleavage planes in the Chevrels are (100) and (110). To obtain sufficient optical surface quality the Chevrel crystals must be polished. We oriented and polished a (111) face of a $Cu_{1.8}Mo_6S_8$ crystal. Though such faces are subject to severe pitting during polishing, there were small areas of sufficient optical quality for the light scattering experiment. By separately measuring the scattered light, polarized parallel and perpendicular to the incident polarization, we differentiated modes belonging to the E_g and A_g representations. We used unoriented polished crystals of $Cu_{3.2}Mo_6S_8$, $PbMo_6S_8$, and $SnMo_6S_8$ in scattering experiments; E_g and A_g symmetries were assigned to peaks in the resulting spectra by looking at the corresponding peaks in the very similar $Cu_{1.8}Mo_6S_8$ spectra. As-grown (100) $BaMo_6S_8$ faces were used and symmetries assigned similarly.

IV. RESULTS AND DISCUSSION

The Raman data are shown in Fig. 1 and 2. The energies and assigned symmetries of the observed peaks are listed in Table II. The strong similarity of the spectra of $SnMo_6S_8$, $PbMo_6S_8$, $BaMo_6S_8$, $Cu_{1.8}Mo_6S_8$, and $Cu_{3.2}Mo_6S_8$ shows that the Raman active phonons are

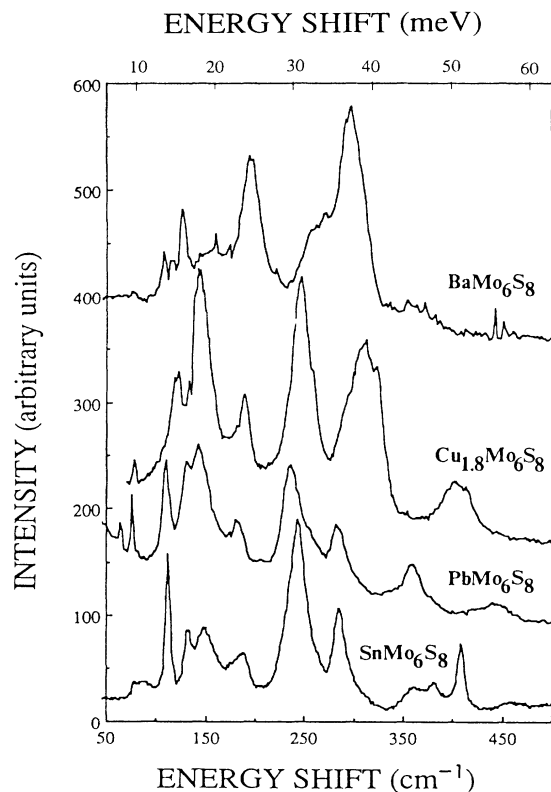


FIG. 1. Raman spectra examples for BaMo_6S_8 , $\text{Cu}_{1.8}\text{Mo}_6\text{S}_8$, PbMo_6S_8 , and SnMo_6S_8 single crystals. The spectra are offset and scaled.

roughly independent of the particular metal atom in the compound.

The superconducting transition temperatures of PbMo_6S_8 , SnMo_6S_8 , $\text{Cu}_{1.8}\text{Mo}_6\text{S}_8$ (Ref. 16), and $\text{Cu}_{3.2}\text{Mo}_6\text{S}_8$ (Ref. 1) are 14.2, 14.2, 10.5 K (transition

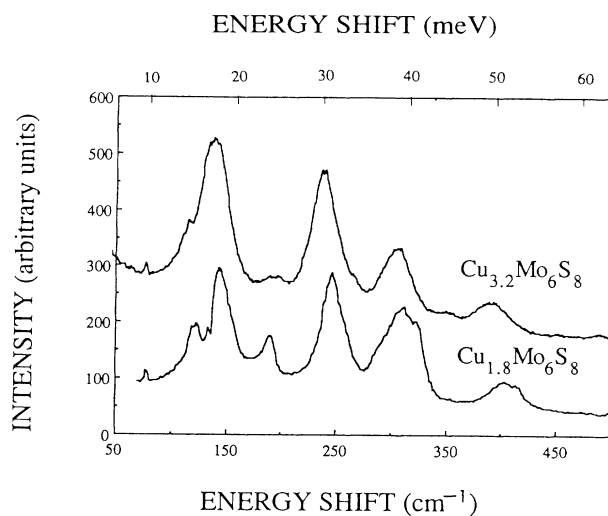


FIG. 2. Raman spectra examples for $\text{Cu}_{3.2}\text{Mo}_6\text{S}_8$ and $\text{Cu}_{1.8}\text{Mo}_6\text{S}_8$ single crystals. The spectra are offset and scaled.

widths ± 0.1 K), and 5 K (uncertainty not listed), respectively. The SnMo_6S_8 and PbMo_6S_8 have an E_g mode at 110 cm^{-1} . The corresponding mode in $\text{Cu}_{1.8}\text{Mo}_6\text{S}_8$ is at 123 cm^{-1} . Theoretical arguments¹⁹ indicate that phonons of low frequency are most effective in electron-phonon coupling and hence more important to superconductivity. Superconducting tunneling data^{14,15} show that phonons in $\text{Cu}_{1.8}\text{Mo}_6\text{S}_8$ at 123 cm^{-1} participate in electron-phonon coupling. The lower frequency of the corresponding mode in SnMo_6S_8 and PbMo_6S_8 may be an important factor contributing to the higher transition temperatures in these compounds.

We note that our phonon data agree with peaks in the electron-phonon interaction weighted phonon density of states identified in the tunneling experiments. The two groups of data are complementary in that the tunneling

TABLE II. Measured frequencies (cm^{-1}) of several Chevrel-phase single crystals. The data shown were taken from multiple spectra of each compound. "Holes" in the table may be due to unresolved peaks lying too near to larger peaks. Assigned symmetries, when unambiguous, are listed. Instrumental resolution: $(3.5 \pm 0.5)\text{ cm}^{-1}$.

| $\text{Cu}_{1.8}\text{Mo}_6\text{S}_8$ | $\text{Cu}_{3.2}\text{Mo}_6\text{S}_8$ | Phonon frequencies (cm^{-1}) | | | Symmetry |
|--|--|---|---------------------------|---------------------------|----------|
| | | SnMo_6S_8 | PbMo_6S_8 | BaMo_6S_8 | |
| | | 85 | | | |
| 123 | | 110 | 110 | 108 | E_g |
| | 140 | 131 | 130 | 125 | |
| 144 | 145 | 145 | 143 | 150 | E_g |
| 190 | 195 | 185 | 180 | 193 | A_g |
| | | 205 | 205 | 220 | |
| 247 | 237 | 242 | 236 | | A_g |
| | | | | 250 | |
| 260 | 268 | 262 | 260 | 265 | E_g |
| 305 | 300 | 285 | 282 | 290 | A_g |
| 321 | 305 | 360 | 360 | 360 | E_g |
| 395 | | 380 | 378 | | E_g |
| 405 | 392 | 405 | 405 | | |
| 415 | | | 442 | | |

peaks are all at energies below 26.5 meV while the Raman peaks extend from 13.5 to about 60 meV.

BaMo₆S₈ has a well-established low-temperature lattice transformation which prevents superconductivity.^{20,21} This is attributed to a Jahn-Teller instability with partial gapping at the Fermi surface.²² The compound does display superconductivity under high pressure.²³ The Raman data show a set of zone-center phonon frequencies which are very similar to those in the other Chevrel compounds measured. The BaMo₆S₈ spectra, however, display a very different pattern of line intensities which we have not been able to explain.

X-ray data² show that in the Cu_xMo₆S₈ system the molybdenum octahedra shrink and the sulfur cubes expand as the copper concentration increases. The most obvious difference between the Cu_{1.8}Mo₆S₈ and Cu_{3.2}Mo₆S₈ spectra is the softening of the 405 cm⁻¹ mode as *x* goes

from 1.8 to 3.2. Such softening suggests that this mode primarily involves motion of the sulfur atoms, since the "force constants" between the sulfur atoms are likely to decrease as the sulfur cubes expand, whereas the "force constants" between the molybdenum atoms should increase as the octahedra shrink.

ACKNOWLEDGMENTS

We would like to thank T. A. Friedmann, B. G. Pazol, M. E. Reeves, and W. H. Wright for their help with the materials preparation. One of us (D.J.H.) thanks the IBM Corporation for financial support. Work supported by the National Science Foundation under Grant Nos. DMR 85-01346 and DMR 84-06473. Characterization of materials was carried out in the Materials Research Laboratory's Center for Microanalysis.

¹Ø. Fischer, *Appl. Phys.* **16**, 1 (1978).

²K. Yvon, in *Current Topics in Materials Science*, edited by E. Kaldis (North-Holland, Amsterdam, 1979), Vol. 3, Chap. 2, p. 53.

³O. K. Andersen, W. Klose, and H. Hohl, *Phys. Rev. B* **17**, 1209 (1978).

⁴L. F. Mattheiss and C. Y. Fong, *Phys. Rev. B* **15**, 1760 (1977).

⁵T. Jarlborg and A. J. Freeman, *J. Magn. Magn. Mater.* **27**, 135 (1982).

⁶S. D. Bader, G. S. Knapp, S. K. Sinha, P. Schweiss, and B. Renker, *Phys. Rev. Lett.* **37**, 344 (1976).

⁷F. Y. Fradin, G. S. Knapp, S. D. Bader, G. Cinader, and C. W. Kimball, in *Superconductivity in d- and f-Band Metals*, edited by D. H. Douglass (Plenum, New York, 1976), p. 137.

⁸S. D. Bader, G. S. Knapp, and A. T. Aldred, *Ferroelectrics* **17**, 321 (1977).

⁹B. P. Schweiss, B. Renker, E. Schneider, and W. Reichardt, in *Superconductivity in d- and f-Band Metals*, Ref. 7, p. 189.

¹⁰S. D. Bader, S. K. Sinha, B. P. Schweiss, and B. Renker, in *Superconductivity in Ternary Compounds I*, edited by Ø. Fischer and M. B. Maple (Springer-Verlag, Berlin, 1982), p. 223.

¹¹R. W. Kimball, L. Weber, G. VanLanduyt, F. Y. Fradin, B.

D. Dunlap, and G. K. Shenoy, *Phys. Rev. Lett.* **36**, 412 (1976).

¹²J. Bolz, J. Hauch, and F. Pobell, *Z. Phys. B* **25**, 351 (1976).

¹³S. D. Bader and S. K. Sinha, *Phys. Rev. B* **18**, 3082 (1978).

¹⁴R. Ohtaki, B. R. Zhao, and H. L. Luo, *J. Low Temp. Phys.* **54**, 119 (1984).

¹⁵U. Poppe and H. Wühl, *J. Low Temp. Phys.* **43**, 371 (1981).

¹⁶W. H. Wright and D. M. Ginsberg, *J. Low Temp. Phys.* **64**, 73 (1986).

¹⁷W. H. Wright, D. J. Holmgren, T. A. Friedmann, M. P. Maher, B. G. Pazol, and D. M. Ginsberg, *J. Low Temp. Phys.* (to be published).

¹⁸R. Flükiger, R. Baillif, and E. Walker, *Mater. Res. Bull.* **13**, 743 (1978).

¹⁹G. Bergmann and D. Rainer, *Z. Phys.* **263**, 59 (1973).

²⁰C. Rossel, M. B. Maple, H. W. Meul, Ø. Fisher, X. J. Zhang, and N. P. Ong, *Physica (The Hague)* **135B**, 381 (1985).

²¹B. Lachal, R. Baillif, A. Junod, and J. Muller, *Solid State Commun.* **45**, 849 (1983).

²²R. C. Laco, S. A. Wolf, P. M. Chaikin, C. Y. Huang, and H. L. Luo, *Phys. Rev. Lett.* **48**, 1212 (1982).

²³P. H. Hor, M. K. Wu, T. H. Lin, X. Y. Shao, X. C. Jin, and C. W. Chu, *Solid State Commun.* **44**, 1605 (1982).